JOURNAL OF GEOPHYSICAL RESEARCH, VOL. 113, F04006, doi:10.1029/2008JF001023, 2008

Continued evolution of Jakobshavn Isbrae following its rapid speedup

Ian Joughin,[1] Ian M. Howat,[2] Mark Fahnestock,[3] Ben Smith,[1] William Krabill,[4] Richard B. Alley,[5] Harry Stern,[1] and Martin Truffer[6,7]

Received 21 March 2008; revised 27 June 2008; accepted 27 August 2008; published 28 October 2008.

[1] Several new data sets reveal that thinning and speedup of Jakobshavn Isbrae continue, following its recent rapid increase in speed as its floating ice tongue disintegrated. The present speedup rate of ~5% a^{-1} over much of the fast-moving region appears to be a diffusive response to the initial much larger speedup near the front. There is strong seasonality in speed over much of the fast-flowing main trunk that shows a good inverse correlation with the seasonally varying length of a short (typically ~6 km) floating ice tongue. This modulation of speed with ice front position supports the hypothesis that the major speedup was caused by loss of the larger floating ice tongue from 1998 to 2003. Analysis of image time series suggests that the transient winter ice tongue is formed when sea ice bonds glacier ice in the fjord to produce a nearly rigid mass that almost entirely suppresses calving. Major calving only resumes in late winter when much of this ice clears from the fjord. The collapse of the ice tongue in the late 1990s followed almost immediately after a sharp decline in winter sea-ice concentration in Disko Bay. This decline may have extended the length of the calving season for several consecutive years, leading to the ice tongue's collapse.

Citation: Joughin, I., I. M. Howat, M. Fahnestock, B. Smith, W. Krabill, R. B. Alley, H. Stern, and M. Truffer (2008), Continued evolution of Jakobshavn Isbrae following its rapid speedup, *J. Geophys. Res.*, *113*, F04006, doi:10.1029/2008JF001023.

1. Introduction

[2] Much of the Greenland Ice Sheet's annual ice loss occurs by calving of icebergs from its many (200+) fast moving (0.5–13 km a^{-1}) outlet glaciers. Since 2000, the speeds of many of these outlet glaciers have increased dramatically (50–150%) [*Howat et al.*, 2005; *Joughin et al.*, 2004; *Luckman et al.*, 2006; *Rignot and Kanagaratnam*, 2006], substantially increasing Greenland's contribution to sea level rise. One of the largest and earliest of these changes was the rapid thinning (up to 15 m a^{-1}) and near doubling in speed of Jakobshavn Isbrae [*Joughin et al.*, 2004; *Thomas et al.*, 2003].

[3] Jakobshavn Isbrae (Sermeq Kujalleqis) is one of Greenland's three largest outlet glaciers, and has the largest drainage basin (Figure 1) on the ice sheet's western margin [*Bindschadler*, 1984; *Rignot and Kanagaratnam*, 2006]. In 1850, near the end of the Little Ice Age, Jakobshavn Isbrae's calving front extended roughly 35 km beyond its current late summer minimum position (Figure 2) [*Csatho et al.*, 2008; *Weidick*, 1995]. Over the next century, a series of retreats moved the calving front back by about 20 km to a point where its position stabilized in the 1950s. For the next 50 years, the calving front maintained a relatively stable mean position with seasonal fluctuations over a range of about 2.5 km [*Csatho et al.*, 2008; *Sohn et al.*, 1998]. During this time, the calving front lay at the end of a 15-km long floating ice tongue that grounded at the present ice front's late summer minimum [*Echelmeyer et al.*, 1991].

[4] In October 1998, the pattern of regular seasonal variation established over the previous several decades changed when the calving front retreated by nearly two kilometers [*Luckman and Murray*, 2005], followed by a further 1.5 km of retreat in September 2002. Despite this summer retreat, the front advanced to its typical multi-decadal maximum extent in the springs of 2001 and 2002. In March 2003, which is typically the time of maximum seasonal extent, the front instead retreated behind even its minimum position from the previous fall [*Alley et al.*, 2005]. The front retreated several more kilometers over the following two months, completing the ice tongue's near-total disintegration [*Joughin et al.*, 2004].

[5] Ice near the grounding line flowed at a rate of 6700 m a^{-1} in 1985, but by 1992 had slowed to 5700 m a^{-1}, a speed that was maintained except for minor variations through the spring of 1997 [*Joughin et al.*, 2004; *Luckman and Murray*, 2005]. The lower regions of the glacier then sped up by

[1]Applied Physics Laboratory, Polar Science Center, University of Washington, Seattle, Washington, USA.
[2]Byrd Polar Research Center, School of Earth Sciences, Ohio State University, Columbus, Ohio, USA.
[3]Institute for the Study of Earth, Oceans, and Space, University of New Hampshire, Durham, New Hampshire, USA.
[4]Cryospheric Sciences Branch, Wallops Flight Facility, Goddard Space Flight Center, NASA, Wallops Island, Virginia, USA.
[5]Department of Geosciences, and Earth and Environmental Systems Institute, Pennsylvania State University, University Park, Pennsylvania, USA.
[6]Geophysical Institute, University of Alaska Fairbanks, Fairbanks, Alaska, USA.
[7]Versuchsanstalt für Wasserbau, Hydrologie und Glaziologie, ETH Zürich, Zürich, Switzerland.

0148-0227/08/2008JF001023$09.00

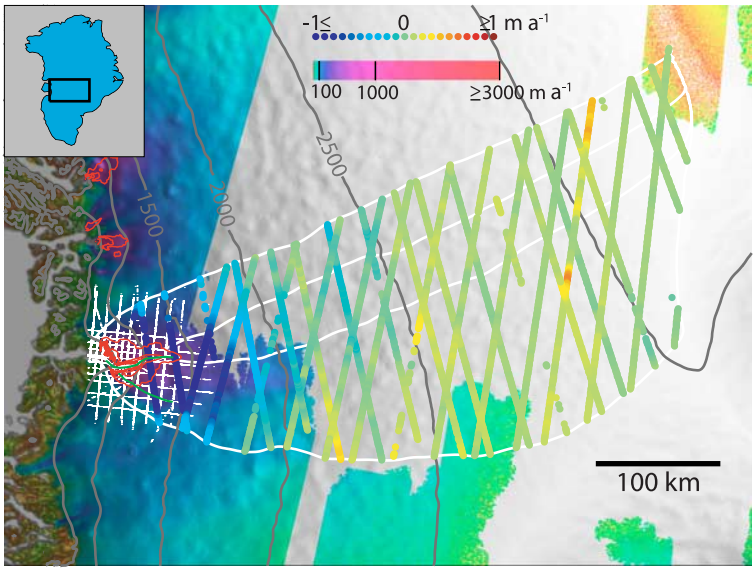

Figure 1. Ice flow speed (lower color bar) over a shaded relief image of a digital elevation model of the study area [*Bamber et al.*, 2001]. Speed up to 2500 m a^{-1} also is shown with 500 m a^{-1} contours (red) and elevation is shown with 500 m contours (dark gray). Colored profiles (top color bar) show rates of surface elevation change derived from ICESAT over the interval from November 2003 to February 2007. White lines denote the overall catchment boundary as well as sections within the catchment. The thin light gray lines show the locations of ATM survey grid and the green lines show the locations of the flow lines used for sampling (see text).

18% in 1998, coincident with the initial ice tongue retreat [*Luckman and Murray*, 2005] and onset of the thinning [*Thomas et al.*, 2003]. The glacier continued to accelerate from 2000 through 2003, reaching a speed of 12,600 m a^{-1} near the grounding line in the spring of 2003, by which time nearly the entire floating ice tongue had disintegrated [*Joughin et al.*, 2004]. Speeds near the front continued to increase through 2004 [*Dietrich et al.*, 2007].

[6] In addition to secular changes, several studies have examined seasonal variation on Jakobshavn Isbrae. *Echelmeyer and Harrison* [1990] found no measurable (>3%) seasonally averaged variation at several points along the glacier from 1985 to 1986. Ten years later during ice tongue's maximum summer retreat, however, the glacier accelerated by 730 m a^{-1} and then slowed through the fall to its early 1990s average speed [*Luckman and Murray*, 2005].

[7] From 2005 to 2007, the speed 4 km inland of the late summer calving front fluctuated seasonally by ±1000 m a^{-1} [*Joughin et al.*, 2008a]. This seasonal fluctuation correlated well with the ice front's current (2004–2007) annual cycle of winter advance (6 km) and summer retreat, with lower velocities occurring with a more extended ice front. In addition to this strong seasonal fluctuation associated with the ice front's position, the speed of the slower regions surrounding the glacier's main trunk fluctuated seasonally (±100 m a^{-1}), with summer speedup correlating well with intensity and duration of surface melt [*Joughin et al.*, 2008a; *Zwally et al.*, 2002].

[8] The initial speedup on Jakobshavn Isbrae produced rapid (1–15+ m a^{-1}) thinning, extending 10s of kilometers inland along the glacier's main trunk [*Krabill et al.*, 2004; *Thomas et al.*, 2003]. Thinning over the trunk should increase the mean surface slope, increasing the gravitational driving stress and ice flow speed upglacier. By this means, thinning and acceleration should diffuse inland, drawing more ice from the ice sheet's interior until a new stable geometry is achieved [*Howat et al.*, 2005; *Payne et al.*, 2004]. At present, it is not clear whether the glacier will evolve quickly toward a new stable geometry or, instead, will continue to retreat inland along the glacier's deep trough [*Clarke and Echelmeyer*, 1996]. Here we examine a time series of velocity and surface elevation to characterize more clearly both the seasonal and secular variation of the early stages of this evolution following the initial, major speedup.

2. Methods

[9] There are many spaceborne and airborne observations of Jakobshavn Isbrae. Here we focus on velocity estimates derived from synthetic aperture radar (SAR) data collected by the Canadian Space Agency's RADARSAT satellite, and laser altimeter data from NASA's Airborne Topographic Mapper (ATM) and Ice Cloud and land Elevation Satellite (ICESAT).

2.1. SAR Methods

[10] We used the speckle-tracking algorithms described by *Joughin* [2002] to produce velocity estimates. In some areas, particularly in summer, the coherence was too poor to obtain good matches using speckle. In these cases, we smoothed the single-look SAR image data with a three-by-three moving average filter to reduce speckle and improve feature-based (e.g., crevasses) matches. We did not use the interferometric phase data since the 24-day interval strongly aliased the results over regions with high strain rates, which composed the majority of the region of interest. To reduce

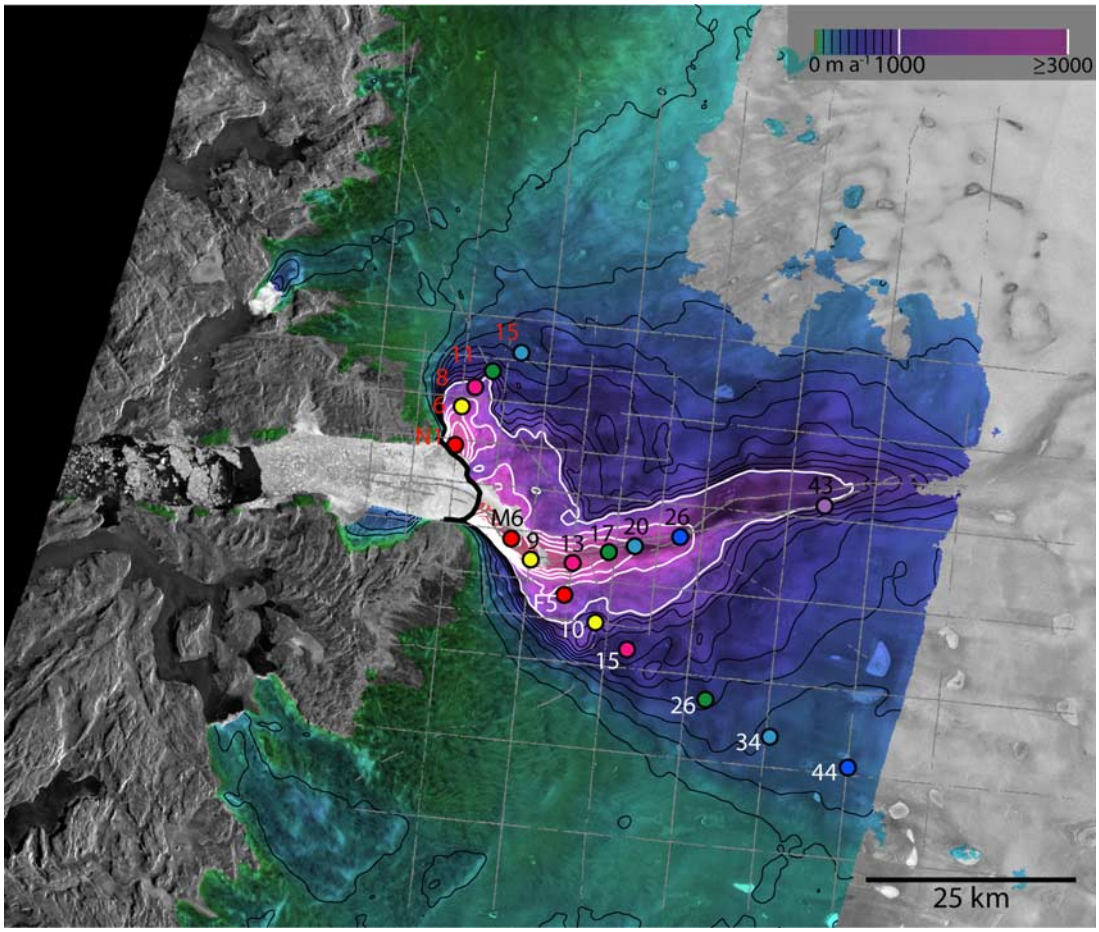

Figure 2. Ice flow speed (color bar) referenced to 1 January 2006 (see text) displayed over a RADARSAT SAR image mosaic from March 2007. Speed up to 900 m a^{-1} is shown with 100 m a^{-1} contours (black) and faster speeds with 1000 m a^{-1} contours (white). Light gray lines show the location of the ATM survey grid. Colored circles indicate locations plotted in Figures 4–6 (see text). The thick black line shows the approximate post-2003 late summer position of maximum retreat.

noise, the speckle-tracked offsets are smoothed to ~800 m resolution, and the final velocity products are posted with 500-m spacing. For the velocity solutions, we determined the interferometric baselines using control points on the wide expanse of exposed bedrock nearby.

[11] We have independent GPS observations from a station 43 km south of the glacier's main trunk [*Das et al.*, 2008; *Joughin et al.*, 2008a]. Fifteen of our speckle-tracked estimates were acquired during the winter period when this station was operating. Comparison of the GPS and In SAR estimates yields a mean difference of 2.1 m a^{-1} with a standard deviation of 6.1 m a^{-1} for an area with a mean speed of 93 m a^{-1} [*Joughin et al.*, 2008a]. These numbers are consistent with the expected level of error from the speckle tracking. We have filtered the data to remove large outliers in the matching procedure, but a few outliers may still exist in fast moving areas. In addition, there are spatially varying errors of 2–3% associated with slope corrections applied to the across-track (range) velocity component [*Joughin*, 2002; *Joughin et al.*, 1998]. Because the SAR imaging geometry is similar for all estimates, these slope-induced errors may influence absolute speeds but tend to repeat, and consequently cancel, so they have little influence on our estimates of speedup.

2.2. ATM Data

[12] NASA's ATM has acquired elevation data on Jakobshavn over a 14-year period [*Krabill et al.*, 1999; *Krabill et al.*, 2000; *Krabill et al.*, 2004]. Here we use data from grid surveys covering a broad region of the glacier, conducted in 1997, 2002, 2005, and 2006 (Figure 1). We smoothed the block elevation data distributed by NASA Wallops, which are the corner elevations of planes fitted to 0.5-s long (time along flight), overlapping subsets of the swath data. These data are initially posted at a time interval of 0.25 s, and we further smoothed them to obtain an along-track spacing of ~2 km. The accuracy of each individual elevation estimate is ~10 cm [*Krabill et al.*, 2004]. With this accuracy and the additional smoothing, we obtain measurement errors for the rate of elevation change of better than $\sigma = 0.1\sqrt{2}/\Delta t$ m a^{-1}, where Δt is the number of years between observations.

[13] The other source of error in dynamic-thinning rate estimates is the interannual variability associated with the surface mass balance (SMB). Approximately 200 km to the south of Jakobshavn Isbrae near Kangerlussuaq, several

sites along the "*K* transect" exhibit a range of mean surface mass balance (SMB) values (−4.0 to −0.7 m a^{-1} water equivalent) for elevations less than 1500 m, but show relatively little variation in the standard deviations of interannual SMB values at each site [*van de Wal et al.*, 2005]. Here we use the mean standard deviation from these sites, $\sigma_{w.e.}$ = 0.56 m a^{-1}, as an estimate for the interannual SMB variability for the area covered by the ATM grid. Most of our region is within the bare ice zone, but the data were acquired in May when the ice was snow covered. Since snow from previous years is lost each summer, each multiyear estimate of elevation change includes both the variability in snow accumulation over the previous winter and the ice equivalent SMB variation over the earlier years. Thus, the uncertainty in determining and elevation change rate resulting from the interannual variability in the surface mass balance is given by

$$\sigma_{\mathrm{SMB}} = \frac{1}{\Delta t}\sqrt{\left(\frac{\rho_{\mathrm{water}}\sigma_{\mathrm{w.e.}}}{\rho_{\mathrm{snow}}}\right)^2 + (\Delta t - 1)\left(\frac{\rho_{\mathrm{water}}\sigma_{\mathrm{w.e.}}}{\rho_{\mathrm{ice}}}\right)^2}, \qquad (1)$$

where the subscripted values of ρ represent densities. This estimate is imperfect because it weights all the variance for 1 year by the density for snow, when in actuality some of this variance includes ablation variability. Lacking better data to partition this variance, however, we use equation 1 with the understanding that it likely overestimates the uncertainty. In using this equation, we used values of 350, 910, and 1000 kg m^{-3} for the densities of snow, ice, and water, respectively [*Paterson*, 1994].

2.3. ICESAT Data

[14] The Geoscience Laser Altimeter System (GLAS) instrument, aboard NASA's ICESAT spacecraft, measures surface elevation along tracks separated by about 30 km over Jakobshavn Isbrae. These measurements were repeated approximately every four months between the fall of 2003 and the early spring of 2007. The accuracy of these data varies with surface conditions, cloud conditions, and the ice surface slope, but after the data were filtered to remove distorted returns caused by surface roughness and atmospheric scattering, the single-shot accuracy is on the order of 0.1–0.2 m [*Howat et al.*, 2008a].

[15] We analyzed these data to obtain rates of elevation change using a multiple-regression algorithm that gives a best fitting surface slope and rate of elevation change for 700-m segments of the ground track [*Howat et al.*, 2008a]. Because data filtering leaves variable numbers of measurements per regression point, and because the accuracy of elevation measurements varies with the surface slope, the formal accuracy of the recovered elevation-change rates varies from one segment to another; only those segments with a formal error less than 0.15 m a^{-1} are used here. Analysis of crossover points, where two tracks have measured elevation-change rates for the same part of the ice sheet, show that the formal errors overestimate the accuracy of the recovered elevation-change rates by about a factor of 4 [*Howat et al.*, 2008a]. Taking this scaling into account, the elevation-change rates used here have a median accuracy of 0.1 m a^{-1}, although the relatively large surface slopes in the lower part of Jakobshavn Isbrae limit the accuracy there to around 0.3 m a^{-1}.

[16] Our analysis of the ICESAT data focuses on the region above 1500 m elevation, which includes the area in the Jakobshavn drainage not covered by the ATM grid. The water equivalent uncertainty for this region should be about $\sigma_{\mathrm{w.e.}}$ = 0.19 m a^{-1} [*van de Wal et al.*, 2005]. For this region, an appropriate expression for the uncertainty associated with the surface mass balance is given by

$$\sigma_{\mathrm{SMB}} = \frac{1}{\Delta t}\sqrt{\Delta t\left(\frac{\rho_{\mathrm{water}}\sigma_{\mathrm{w.e.}}}{\rho_{\mathrm{firn}}}\right)^2} = \left(\frac{\rho_{\mathrm{water}}}{\rho_{\mathrm{firn}}}\right)\frac{\sigma_{\mathrm{w.e.}}}{\sqrt{\Delta t}}. \qquad (2)$$

A midrange value of ρ_{firn} = 600 kg m^{-3} [*Paterson*, 1994] yields σ_{SMB} 0.18 m a^{-1} for the slightly longer than 3-year period covered by the ICESAT observations. Combining this with the measurement uncertainty described above, yields an uncertainty in thinning rates of 0.21 m a^{-1}.

3. Results

[17] The time series we have assembled of RADARSAT velocities and ATM and ICESAT elevation differences provide an exceptionally clear view of a large outlet glacier's evolution following a major speedup. Figures 1 and 2 show the locations of these data, which are described throughout the remainder of this section.

3.1. Velocity

[18] With the exception of a few missed acquisitions, fine beam (∼10-m resolution) RADARSAT data were acquired every 24 days between September 2004 and August 2007 along overlapping tracks covering most of Jakobshavn Isbrae's fast-moving area. This coverage produced an average of 31 image pairs per track (94 total). In areas with overlap, which includes the area 15 km upstream of the grounding line, there are up to 72 independent estimates of velocity over the 3-year period.

[19] To examine the variation in the glacier's speed, we performed a linear fit at each point where 12 or more measurements were available. This method has the advantage of using all of the estimates to provide a secular trend, which is less sensitive to noise than a simple difference of the first and last estimates, and is less likely to alias seasonal variability. Figure 2 shows the results from these linear fits, which produce estimates of the speed referenced to 1 January 2006 (the intercepts, because we used that date as the zero of the timeline). Unfortunately we have a far more limited set of observations prior to 2004, so we compute speedup for earlier periods by differencing pairs of velocity estimates.

[20] Figure 3 shows the annual rates of speedup for three periods: mid-1990s–2000, 2000–2004, and 2004–2007. For the mid-1990s data, we averaged estimates from 1992, 1994, and 1995 when speeds were nearly constant [*Joughin et al.*, 2004]. Time series of velocity data from the 1990s indicate that the initial speedup on Jakobshavn Isbrae began relatively abruptly in about July 1998 [*Luckman and Murray*, 2005]. Thus, we have assumed that our mid-1990s estimate is representative of the speed in the early summer of 1998 and have approximated the 1998–2000 speedup

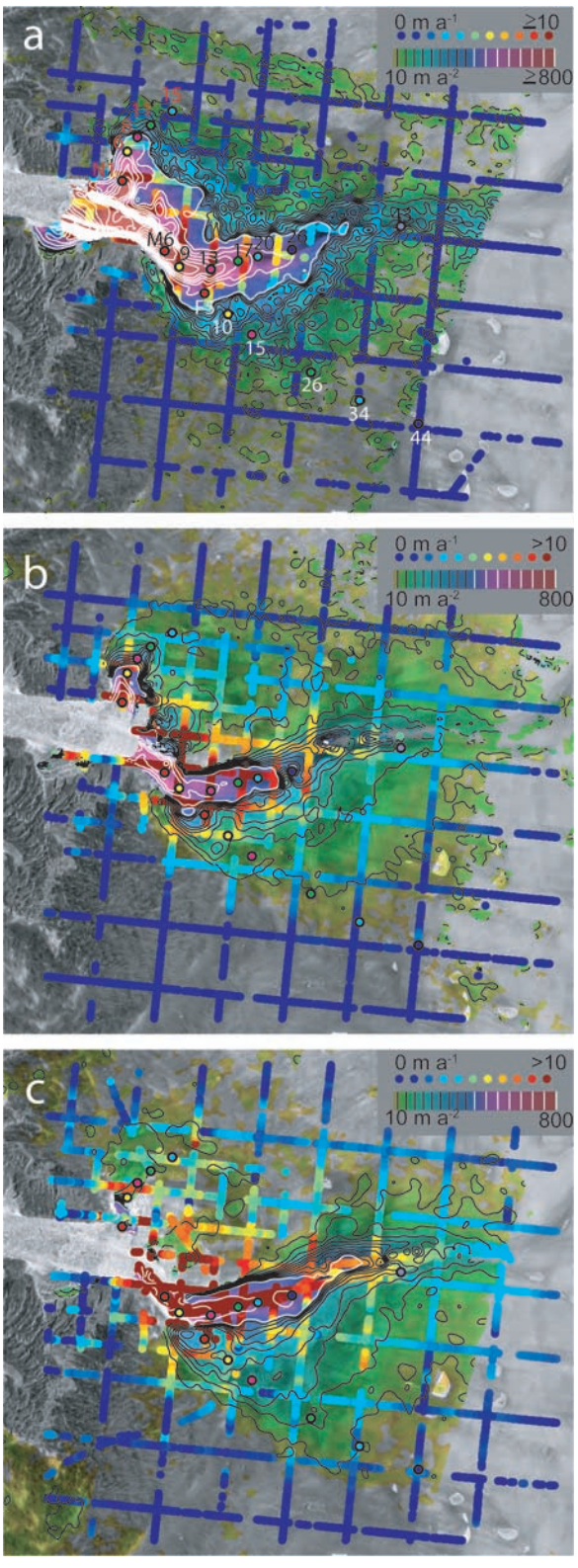

Figure 3. Thinning (colored lines) and rates of speedup plotted over SAR mosaic from March 2007. (a) The speedup rates are from 1998 to 2000, on the basis of the assumption the speedup began in mid-1998 (see text) and thinning rates are averaged over the period from 1997 to 2002. (b) Average rate of speedup from 2000 to 2004 and thinning from 2002 to 2005. (c) Average rate of speedup from 2004 to 2007 and thinning from 2005 to 2006.

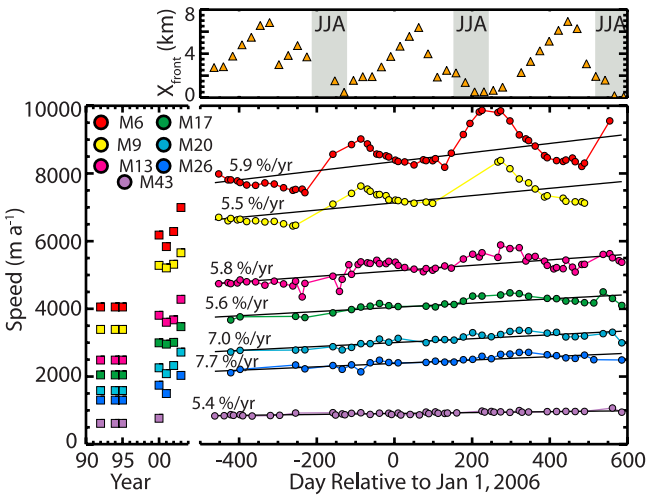

Figure 4. Speed at several points (Figure 2, M6–M43) along the main trunk of Jakobshavn Isbrae. (left) Speed from 1992 to 2003 [*Joughin et al.*, 2004]. (right) Speed from 2004 to 2007 with linear trends (black). (top) Relative position of the calving front from 2004 to 2007 (advance indicated by increasing value). Gray shading indicates the June-July-August (JJA) period.

rates by dividing the velocity change between the mid 1990s and 2000 by a time interval of just over 2 years (summer 1998 to fall 2000). Although this provides an approximate average rate of speedup, the actual rate was likely highly variable during this period as the ice shelf weakened and disintegrated [*Luckman and Murray*, 2005].

[21] The mid-1990s estimate was computed from ERS images acquired 1 to 3 days apart [*Joughin et al.*, 2004], making this result much noisier than subsequent estimates computed from 24-day RADARSAT data. Although this noise is evident in the much more irregular contours in Figure 3a, it is clear that rates of speedup are by far the greatest from 1998 to 2000, particularly along and immediately adjacent to the main trunk. While the post-2000 rates of speedup are smaller on the trunk, the speedup (e.g., 10 m a^{-2} contour) appears to have migrated inland on the south side of the glacier during this period. In contrast, on much of the north side there is little speedup after 2000.

[22] Figure 4 shows speed at several points along the glacier's main trunk at the locations shown in Figure 2 (M6–M43). The numbering of these points indicates the approximate distance in kilometers from the ice front's post-2003 late summer minimum position. The left side of the plot, which shows the annual estimates from 1992 to 2003 [*Joughin et al.*, 2004], indicates that some further speedup occurred between summer 2003 and fall 2004. The right side of the plot shows linear fits (black lines) to the 2004–2007 time series. Also shown are the rates of speedup in % a^{-1} (the trend line's slope divided by its y intercept). The rates of speedup are all relatively consistent along the glacier's main trunk, lying in the range from 5.4 to 7.7% a^{-1}.

[23] The speed at M6 shows a strong seasonal variation ($\sim \pm$ 1000 m a^{-1}) about the trend line, similar to that described for a nearby location extracted from the same time series of velocity grids [*Joughin et al.*, 2008a]. This

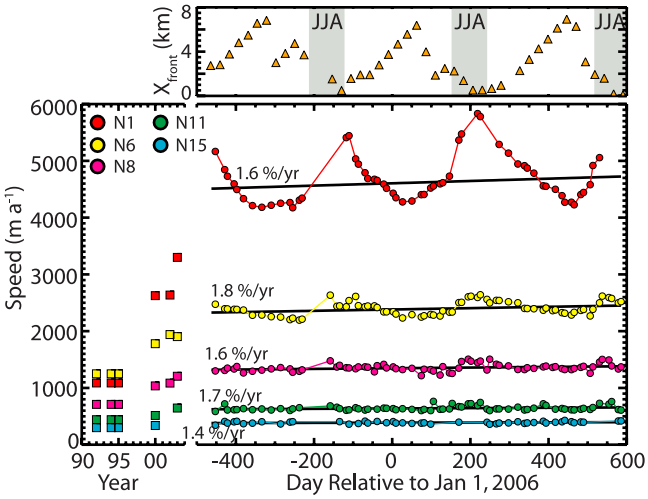

Figure 5. Speed at several points (Figure 2, N1–N15) along the north branch of Jakobshavn Isbrae. (left) Speed from 1992 to 2003 [*Joughin et al.*, 2004]. (right) Speed from 2004 to 2007 with linear trends (black). (top) Relative position of the calving front from 2004 to 2007 (advance indicated by increasing value). Gray shading indicates the June-July-August (JJA) period.

variation is discernable at other points, and the seasonal amplitudes decrease with increasing distance inland. Only at the farthest point inland, M43, is there no visible sign of this seasonal fluctuation. As noted earlier [*Joughin et al.*, 2008a], the speed variation on the glacier's lower regions correlates (negatively) well with the ice front's seasonal position (Figure 4 (top)).

[24] Figure 5 shows a time series of speed at five points along the Jakobshavn Isbrae's north branch (N1–N15). The speedup trend is more modest along this branch (1.4–1.8% a^{-1}), which is consistent with the maps shown in Figure 3 that indicate little post-2004 speedup. As with the main branch, there is a seasonal variation in speed that correlates well with the ice front position.

[25] Figure 6 shows the speed at several points (F5–F44) along an approximate flow line that joins the glacier's south side near the location where it "doglegs" (Figure 2). Here the points' numerical designation gives the distance in kilometers from the center of the main trunk. Over the flow line's first 26 km, the rate of speedup ranges from 4.0 to 5.9% a^{-1}, which is similar to the values on the main trunk. The rate of speedup begins to decline (3.6% a^{-1}) at point F34 and by point F44 there is only negligible speedup (1.5% a^{-1}). A correlation between speed and the seasonal variation of the ice front position is clearly discernable at F5, but it dies out completely by point F10. A summer speedup of roughly 75 to 150 m a^{-1} is visible at points F10–F26, particularly near day 200, which corresponds roughly with the expected peak in surface melt [*Joughin et al.*, 2008a]. At F34 and F44, there are no summer data with which to determine whether the surface-melt-induced speedup extends this far inland. Although there are slight suggestions of surface-melt-induced speedup in Figures 4 and 5, the magnitude of any such speedup is small relative to both the glacier's mean speed and to the larger ice-front-related pattern of seasonal variation.

3.2. ATM Elevation Changes

[26] Figure 3 shows the ATM-determined thinning rates for the intervals that most closely match the periods over which we have velocity change estimates. As with the velocity estimates, the first ATM survey in 1997 occurred before the speedup began in 1998 [*Luckman and Murray*, 2005]. In this case, however, we computed the thinning rates using the actual 5-year interval between measurements. Because the speedup did not begin until about a year later, this may underestimate the average thinning rates by 25–30% during the period when the glacier's speed was increasing. Results from *Thomas et al.* [2003] on a more limited set of ATM data just above the grounding line show that the thinning rates from 1998 to 1999 were about a factor of three larger than the corresponding rates from 1997 to 1998. Prior to 1997, their results show that the ice in this region had been thickening slightly.

[27] Our results show strong thinning (>10 m a^{-1}; σ = 0.4 m a^{-1}) near the front over the interval from 1997 to 2002 when Jakobshavn Isbrae was speeding up rapidly. Thinning at rates greater than about a meter per year is largely confined to the fast-flowing region on and immediately adjacent to the glacier's main trunk. Figure 7 shows thinning rates along a flow line (Figure 1) down the glacier's main branch at the points where it intersects the ATM gridlines. From 1997 to 2002, the ice at the upper end of the profile thinned at ~1.5 m a^{-1}, with steadily increasing rates toward the ice front, consistent with the pattern of increasing along-flow strain rates. Figure 8 shows thinning along the flow line used to define the points F5–F44. Figure 8 indicates that there was little or no thinning from 1997 to 2002 near the upper ends of the ATM grid in regions well away from the glacier's main trunk.

[28] From 2002 to 2005, thinning rates near the front (Figures 3 and 7) were similar in magnitude to that over the period from 1997 to 2002. At the farther inland sections of the main trunk, however, thinning increased substantially over time (Figure 3b), with thinning rates more than doubling at 50 km from the grounding line (Figure 7).

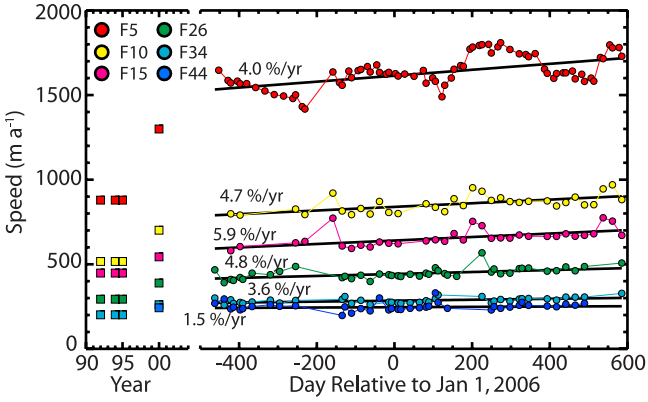

Figure 6. Speed at several points (Figure 2, F5–F44) along a flow line that intersects the main trunk from the south. (left) Speed from 1992 to 2000 [*Joughin et al.*, 2004]. (right) Speed from 2004 to 2007 with linear trends (black).

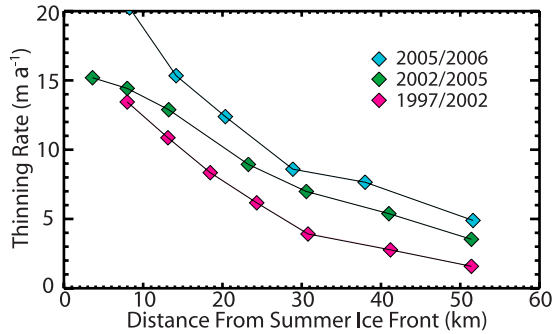

Figure 7. Thinning rates at the locations (plot symbols) where an approximate flow line down the main trunk of Jakobshavn Isbrae (Figure 1) intersects the ATM survey grid. Note that because repeat ATM data coverage is different for each period the points where the flow line intersects the gridlines also differ.

Thinning also began to radiate laterally outward from the main trunk in a pattern similar to the speedup. For example, thinning at rates (Figure 3b, light-to-dark blue transition) of about 3 m a^{-1} (σ = 0.6 m a^{-1}) roughly corresponds to the 10 m a^{-1} 2000–2004 speedup contour. While there was little or no thinning prior to 2002 along the section between 40 and 50 km of the southern flow line (e.g., points F5–45 in Figure 2), this section thinned at rates of 1 to 2 m a^{-1} from 2002 to 2005 (Figure 8).

[29] Overall, the 2005–2006 ATM thinning data suggest sustained thinning that continues to migrate inland. Thinning rates along the south side of the glacier increased by about 1–2 m a^{-1} (Figure 8). While these values are close to the uncertainty for the 1-year observations (σ = 1.6 m a^{-1}), the results suggest that the 2002–2005 thinning rates are at least sustained, and may also be increasing. Increased thinning in this region would be consistent with the inland migration of the speedup discussed above. On the glacier's north side, however, thinning appears to have increased although there is little additional speedup. The 2005–2006 thinning rates also appear to have increased along the main trunk. At distances of more than about 50 km from grounding line, the 1.5–2.5 m a^{-1} increase in thinning rate is slightly larger than the increase along the southern flow line. Nearer the ice front, there is an approximately 5 m a^{-1} increase in thinning from 2005 to 2006. While some of this increase appears real, the 2005 and 2006 ATM flight lines lie more toward the center of the glacier near the ice front (Figure 3), which may bias the results toward slightly higher thinning rates. In addition, thinning rates for this region may be more variable than for regions farther inland because of the ice front's 6-km annual migration. Inspection of a more limited set of ATM acquisitions from 2007 (not shown), suggests 2-year thinning rates near the front (2005–2007) are not appreciably different from the 2002 to 2005 period.

[30] We gridded the ATM elevation change data shown in Figure 3 to determine volume change over the 9016 km^2 area covered by the ATM surveys. In computing error estimates we have assumed that the SMB uncertainty is regional, and thus does not average out spatially when integrating over the area covered by the ATM grid. The rate of volume change from 1997 to 2002 was -9 ± 4 km^3 a^{-1}, which is similar to that calculated earlier [*Krabill et al.*, 2004]. The lower part of the glacier was thickening prior to 1997 [*Thomas et al.*, 2003], so the actual change in mass balance was likely somewhat greater. From 2002 to 2005 the magnitude of this rate increased to -17 ± 5 km^3 a^{-1}, which is consistent with an estimate for 2005 of -16 km^3 a^{-1} [*Rignot and Kanagaratnam*, 2006]. With substantial uncertainty, the magnitude of the volume change rate increased to -23 ± 14 from 2005 to 2006.

[31] The flux across the grounding line was estimated at 23.6 km^3 a^{-1} in 1996 with thickening of 6.4 km^3 a^{-1} [*Rignot and Kanagaratnam*, 2006]. Using these numbers along with ATM thinning rates yields a flux across the grounding line of 47.5 km^3 a^{-1} averaged over the period from 2002 to 2005. This likely is a low estimate because it neglects the additional thinning in the interior outside the ATM grid. Neglecting thinning at the ice front and assuming speedup of ~5 to 6% a^{-1} near the grounding line (Figure 4), this flux should have increased by 4.9 to 5.9 km^3 a^{-1} from the 2002–2005 to the 2005–2006 ATM interval, which, despite the large uncertainty, agrees well with increased thinning of 6 km^3 a^{-1}.

3.3. ICESAT Elevation Changes

[32] With ICESAT there are only sufficient observations to determine an elevation change trend (Figure 1) for a single period (November 2003 to February 2007). These data show appreciable thinning (e.g., >0.21 m a^{-1}) extending up to elevations of about 2000 m (Figure 1), with little detectable thinning farther inland. Thinning rates between the 2000-m contour and the ATM grid's upper extent lie within the range of about 0.2 to 1.0 m a^{-1}, with the strongest thinning concentrated on the southern portion of the basin.

4. Discussion

4.1. Stages of Recent Change

[33] The observations we present here and those from earlier studies [e.g., *Fastook et al.*, 1995; *Joughin et al.*, 2004; *Luckman and Murray*, 2005] span more than two decades, which can be divided into four distinct periods. The first period includes the mid-1980s, when the glacier likely flowed at about 6700 m a^{-1} near the grounding line [*Fastook et al.*, 1995]. During this period there was no significant seasonal fluctuation in flow speed [*Echelmeyer*

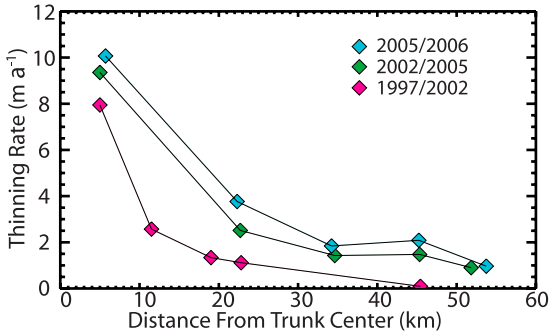

Figure 8. Thinning rates at the locations where the flow line from the south (Figure 2, F5–F44) intersects the ATM survey grid.

and Harrison, 1990], perhaps because the floating ice front maintained a relatively stable position [*Sohn et al.*, 1998].

[34] The second period began sometime between 1986 and 1992, when the glacier slowed by about 1000 m a^{-1} near the grounding line [*Joughin et al.*, 2004] and thickened substantially near the ice front [*Csatho et al.*, 2008; *Thomas et al.*, 2003]. During the times when observations are available for this period (1992–1998), the glacier's speed remained relatively stable [*Joughin et al.*, 2004; *Luckman and Murray*, 2005]. An exception to this stability occurred when there was a summer speedup in 1995 (770 m a^{-1}), which may have been a response to the ice front calving back slightly farther than in other summers during this period [*Luckman and Murray*, 2005]. Other than this event, there appears to have been little seasonal variability over this slow period.

[35] The third period began in about mid-1998 and lasted until fall 2003, and covers the interval when the glacier began to speed up rapidly as the ice shelf began to thin, weaken, and disintegrate [*Joughin et al.*, 2004; *Luckman and Murray*, 2005; *Thomas et al.*, 2003]. Over this period, the glacier's speed increased by roughly 70% over the first 20 km along the main trunk (Figure 4, M6–M20). Speedup during this period was not uniform. *Luckman and Murray* [2005] show a step change in speed in 1998, followed by a nearly yearlong period of little change, prior to a large speedup in 2000. The sparsely sampled data from 2000 to 2003 (Figure 4) also suggest nonuniform speedup, and a minor slowdown in 2001. The range of variation over this interval, however, is comparable to the seasonal variation evident in later years. This may explain the slower 2001 speeds, which were measured in May. Unfortunately, we do not have sufficient data to resolve the degree of seasonal variation during the ice tongue's final breakup.

[36] The last period, which extends from about late 2003 to present, corresponds to the time after the main ice shelf had disintegrated and the ice front had switched to its present cycle of seasonal advance and retreat. The data for this period show a linearly increasing speedup over much of the glacier's fast moving area (Figures 4–6) at rates of about 5% a^{-1}. Superimposed on this speedup is a pattern of strong seasonal fluctuation that is largest in the vicinity of the ice front and continues upglacier over a distance that represents about 10 to 20 ice thicknesses [*Clarke and Echelmeyer*, 1996]. In addition, a smaller magnitude ($\sim$100 m a^{-1}), shorter-duration speedup is in phase with summer surface melting [*Joughin et al.*, 2008a; *Zwally et al.*, 2002], which is most apparent in areas where there is no other seasonal variation (Figure 6). It is important to note that this apparent melt-related signal only occurs during the melt season and appears to be a response to increased basal lubrication independent of the larger speedup on the main trunk, which correlates with the ice tongue's extent [*Joughin et al.*, 2008a; *Zwally et al.*, 2002].

4.2. Loss of Buttressing Resistance

[37] Earlier studies have suggested that loss of the buttressing ice tongue produced the initial speedup [*Joughin et al.*, 2004; *Thomas*, 2004]. This hypothesis is complicated by the fact that the rate of speedup was greatest while much of the ice shelf was still visibly in place (1998–2003) [*Csatho et al.*, 2008]. Several factors, however, suggest that while much of the ice tongue was still in place in 2000, it likely provided far less buttressing resistance than it did in earlier years.

[38] One of these factors is the 36 m decrease in elevation of the ice tongue between 1997 and 2001 measured by *Thomas et al.* [2003] from ATM data, which indicates that the floating ice thinned by $\sim$320 m ($\sim$40%). This degree of thinning should have produced a substantial reduction in the potential backstress that could be provided by the floating ice tongue.

[39] Another factor may be related to the large rifts near the grounding line that were visible on the north side of the fjord in 2000 and that were not visible in images from the mid-1990s (Figure 9, white box). *Thomas et al.* [2003] referred to this region as the "rumples" and suggested that the grounded ice in this region thinned enough to reach flotation. The presence of the rifts supports this hypothesis since large basal rifts should only propagate to the surface when ice is floating or near flotation [*van der Veen*, 1998a]. Similar rifts have been associated with the glacial earthquakes that coincide with large calving events on Helheim and Kangerdlugssuaq glaciers on Greenland's east coast [*Joughin et al.*, 2008b]. For Jakobshavn Isbrae, 11 of the 13 glacial earthquakes detected from 1993 to 2005 occurred in 1998 and 1999 [*Tsai and Ekstrom*, 2007], which corresponds to the period when rapid speedup began and when the large rifts likely formed. Furthermore, the 1998 earthquakes occurred in late June–July, which coincides well with the May–August 1998 period when the initial speedup occurred [*Luckman and Murray*, 2005]. Thus, for the north side of Jakobshavn Isbrae, as originally suggested by *Thomas et al.* [2003], an area of up to several square kilometers may have thinned and ungrounded during the period of rapid speedup from 1998 to 2000. In addition to the loss of resistive stress associated with the ungrounding, the rifts likely weakened the ice tongue so that it produced much less resistance to flow along the fjord's northern side.

[40] On the fjord's south side, the ice front calved back in 2000 to a point that was nearly even with the stabilizing southern ice rumple (Figure 9, white circle) [*Echelmeyer et al.*, 1991; *Thomas et al.*, 2003]. After 2000, the calving front progressively retreated even farther from any stabilizing influence provided by this rumple. There were periods in the springs of 2001 and 2002 when the calving front extended beyond this ice rumple while maintaining speeds of greater than 9000 m a^{-1}. During these periods, however, the ice tongue was detached from much of the ice adjacent to the rumple, unlike the mid-1990s when this area supported strong lateral shear. Thus, the combined weakening along the northern and southern sides of the fjord, the loss of grounded ice, and the substantial thinning of the ice shelf all suggest a large reduction in resistive stresses by fall 2000, even though the ice tongue seasonally advanced over the following three winters to nearly the full extent it had maintained over the last several decades.

[41] The initial rapid speedup from 1998 to 2003 (Figure 4) coincides well with an apparent reduction in resistive stress as grounded and floating ice were lost. In addition, the magnitudes of the speedup are roughly consistent with model-based predictions [*Thomas*, 2004]. Perhaps the best evidence for the hypothesis that the speedup resulted from the ice tongue's demise [*Joughin et al.*, 2004; *Thomas et al.*,

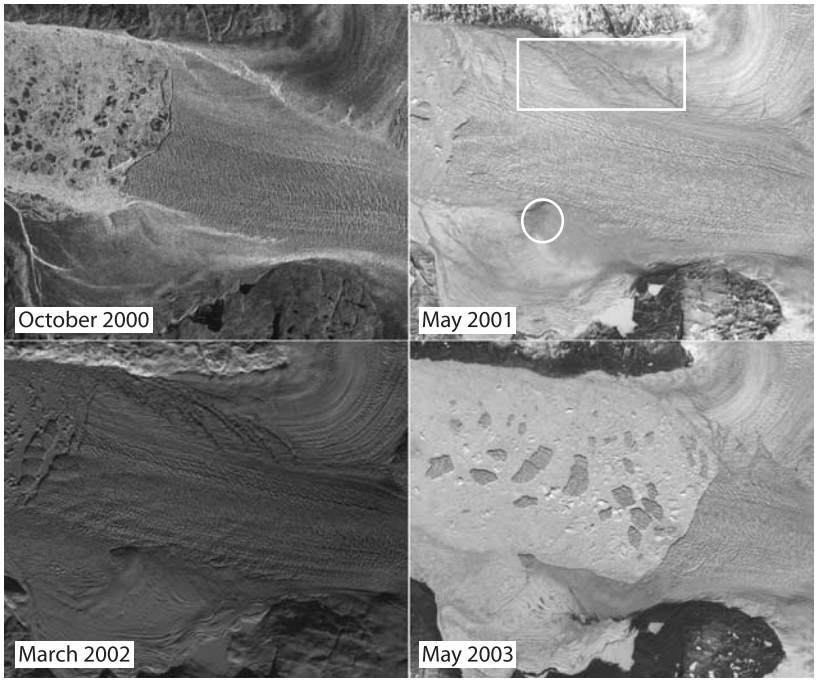

Figure 9. Sequence of images showing the state of the Jakobshavn Isbrae's ice tongue during its breakup and retreat. The white box and circle show locations referenced in the text.

2003; *Thomas*, 2004] comes from the current pattern of seasonal speedup (Figures 4 and 5). While it is unclear to what extent the seasonally varying ice front is grounded, resistive stress should increase during the winter advance as more ice comes in contact with the walls and base of the fjord. Near the front at M6 (Figure 4), the peak-to-peak amplitude of the seasonal swing ($\sim$2000 m a^{-1}) is just under half the value of speed (4055 m a^{-1}) at this point prior to speedup. While it is difficult to perform a quantitative analysis, a qualitative evaluation suggests the resistive stress produced by the seasonally advanced ice front must be substantially less (<50%) than that provided by the fully extended ice shelf in the mid-1990s. Thus, the magnitude of Jakobshavn Isbrae's speedup as its ice tongue disintegrated is well within the range of that implied by the response to the lesser-amplitude seasonal forcing. This also is consistent with a strong correlation between speed and ice front position for a large sampling of glaciers along Greenland's east coast [*Howat et al.*, 2008b].

4.3. Evolving Geometry

[42] Despite a large seasonal variation in its position, the ice front calved back to nearly the same position each summer from 2004 to 2007, suggesting little further loss of resistive stress from mean annual ice front retreat. The strong thinning that accompanied the speedup is widespread over the basin at elevations below 2000 m (Figure 1) and is directly influencing both thickness, H, and surface slope, α, both of which influence flow speed through the driving stress [*Paterson*, 1994]. Relative changes in surface slope are larger than in thickness in most places, and the influence of the surface slope change on ice flow is calculated to explain at least much of the change in ice flow speed, as shown next.

[43] For sheet flow with ice frozen to the bed, flow speed, U, is proportional to α^n and H^{n+1}, where n is the exponent in Glen's flow law [*Paterson*, 1994]. For sliding where basal shear stress balances the full driving stress, sliding laws yield a relation such that $U \sim \alpha^n$ with $n = 2$ or 3 [*Paterson*, 1994]. Other sliding theories suggest n approaches infinity to yield behavior close to perfect plasticity or even velocity-weakening characteristics in cases of high sliding speeds and low effective pressures [*Schoof*, 2005]. The dependence on H is more complicated for sliding because it influences both the driving stress and the effective pressure, and these variables have opposite effects on the velocity [*Pfeffer*, 2007].

[44] If $U \sim \alpha^n$, either through sliding or internal deformation, then for a small percentage change $\Delta\alpha/\alpha$ the corresponding proportional speedup is $\Delta U/U = n\Delta\alpha/\alpha$. From the thinning rates averaged over the three profiles shown in Figure 7, we estimated normalized rates of slope change of 1.8% a^{-1} from 10 to 33km and 1.0% a^{-1} from 30 to 52 km, which yield corresponding rates of speedup of 5.4% a^{-1} and 3.0% a^{-1} if we assume $n = 3$. For comparison, the mean rate of speedup for points M6–M26 is 6.25% a^{-1}. At M46, steepening can account for slightly more than half the total speedup, though the section over which thinning was determined extends several km farther inland where rates of acceleration may be smaller. We performed a similar analysis for the thinning rates shown in Figure 8. For the section that includes F5 through F26, the slope changed at a rate of 1.5% a^{-1} to yield an estimated speedup rate of 4.5% a^{-1} compared to the observed average rate of 4.8% a^{-1}. Toward the upper end of the profile, thinning rates yielded an estimated speedup of 1.8% a^{-1}, while the observed speedup at F34 and F44 averaged 2.5% a^{-1}. Thus, with an exponent of $n = 3$, the slope-

change rates caused by the thinning can account for most of the speedup observed since 2004. The strong internal deformation believed to occur near the bed [*Clarke and Echelmeyer*, 1996; *Luthi et al.*, 2002] and strong shear in the margins, which on the narrow main trunk have area comparable to that of the bed, suggest that a value of $n = 3$ is appropriate. Where stresses are large, a higher exponent (e.g., $n = 4$) for the flow law might apply [*Goldsby and Kohlstedt*, 2001; *Weertman*, 1983]. Even with an exponent of 2, as some sliding laws suggest, steepening can still account for roughly half of the post-2004 speedup.

[45] Thickness is poorly known for Jakobshavn Isbrae's main channel, but seismic observations suggest values 1500 to 2500 m along much of the channel [*Clarke and Echelmeyer*, 1996]. A central value of 2000 m yields relative thinning rates of 0.25% a^{-1} and 0.5% a^{-1} for the upper and lower sections, respectively, of the profile shown in Figure 7. It is difficult to say, however, how this thinning affects flow. For sheet flow, thinning would tend to slow flow by reducing the driving stress. Alternatively, it could cause speedup by reducing lateral resistive stresses or reducing the effective pressure [*Pfeffer*, 2007]. While it is difficult to identify how the rate of thickness change would influence flow, the magnitudes of the relative rates of change are about a factor of 3 smaller than the rates of slope change. This difference, along with the good spatial agreement between the speedup and the slope-change rates, suggest that slope changes associated with thinning gradients are the dominant influence on the current speedup. In terms of kinematic wave theory, this suggests that diffusion dominates advection [*Alley and Whillans*, 1984; *Bindschadler*, 1997; *Paterson*, 1994].

[46] The rapid speedup on Jakobshavn followed by the more gradual diffusion inland suggests a progression similar to that revealed by numerical models and observations of Pine Island Glacier in Antarctica [*Dupont and Alley*, 2005; *Joughin et al.*, 2003; *Payne et al.*, 2004] and hypothesized for Helheim Glacier along Greenland's east coast [*Howat et al.*, 2005, 2007]. In these cases, an initial loss of resistive stress near the grounding line produces a nearly instantaneous dynamic response as the ice speeds up to produce the horizontal stress gradients necessary to restore force balance, producing rapid thinning over an area that extends inland roughly 10 to 20 ice thicknesses. This is soon followed by a more gradual speedup that diffuses inland as the initial thinning steepens slopes, further increasing speed [*Howat et al.*, 2005; *Joughin et al.*, 2003; *Payne et al.*, 2004].

4.4. Sikkusak and Calving

[47] The data in Figure 4 show a strong annual variation in calving with almost no calving over much of the winter as the ice front advanced. This advance was followed by rapid calving through the spring and summer as the ice front retreated. Calving rates also varied seasonally from the 1960s to the 1990s, with substantially higher spring and summer iceberg production [*Sohn et al.*, 1998]. A similar seasonal variation in calving rates also occurs for Helheim and Kangerdlugssuaq glaciers [*Joughin et al.*, 2008b; *Luckman et al.*, 2006]. Because the ice front's position and the ice tongue's stability are directly influenced by the calving rate, it is likely that the processes that control the seasonal calving cycle may also influence the interannual variability.

[48] Two mechanisms have been proposed to explain the seasonality in the calving for Jakobshavn Isbrae [*Sohn et al.*, 1998]. The first of these assumes that seasonal surface melt fills crevasses near the calving front, causing hydrofracturing that increases calving rates [*Scambos et al.*, 2000; *van der Veen*, 1998b]. The second assumes that the icebergs frozen together by sea ice, referred to here as sikkusak [*Jennings and Weiner*, 1996], in the fjord influences near-calving front stresses in such a way that it slows winter calving but likely has negligible direct influence on the glacier's overall force balance [*Reeh et al.*, 2001]. In the case of Jakobshavn Isbrae, it is possible that the formation of sikkusak in the fjord provides sufficient resistance to prevent fractured ice from rotating away as icebergs, or icebergs from floating away from the glacier terminus.

[49] To investigate these hypotheses, Figure 10 (top) compares the ice front position with the mean monthly temperatures at Egedesminde (Aasiaat), 85 km southwest of where the fjord enters Disko Bay. Figure 10 also shows the periods (green lines) when the speckle-tracked data indicate that the sikkusak in the fjord is sufficiently frozen to behave almost rigidly, as the advancing ice front pushes it down the fjord with little or no relative motion between blocks of glacial ice (Figure 10 (left)). Midwinter gaps in this record indicate either a data gap, or motion too rapid to fall within the speckle tracker's bounds, such as would occur during a rapid flushing of ice from the fjord (e.g., Figure 10, March image).

[50] Figure 10 indicates that each year the ice front began to advance in late September at about the same time mean air temperatures fell below freezing. This coincides well with when the fjord freezes to form sikkusak that begins to move nearly rigidly as indicated by the speckle-tracked data. Thus, the timing of the advance's onset is consistent with either the melt or sea-ice related hypothesis. For all three winters shown in Figure 10, however, the ice front begins to calve back rapidly in February/March, when the sikkusak breaks out (see below), but while mean surface temperatures are well below freezing. Furthermore, there is relatively little change in the calving rate roughly two months later when surface temperatures do rise above freezing. Thus, while we cannot rule out some lesser influence of surface melt on calving, the observations indicate that it is not the dominant control. Instead, the data suggest that the sikkusak acts as a major control on the calving rate [see also *Reeh et al.*, 2001].

[51] Because of high seasonal calving rates, the fjord's entire length is choked with icebergs at the end of each summer, many of which are obstructed from flowing into Disko Bay by a shoal at the fjord's mouth [*Echelmeyer et al.*, 1991]. Falling temperatures each September form sea ice that bonds icebergs, producing a rigid barrier that has to be pushed along as the front advances. At some point along the fjord, an "ice dam" forms because of either a narrowing or shallowing of the fjord, with little glacial ice advancing past this point (Figure 10 (left)). Each winter between 2004 and 2007, a large area of open water formed on the seaward side of the constriction by midwinter, allowing ice to clear from the fjord (Figure 10, dark area in the January and February images). With the ice cleared from its seaward

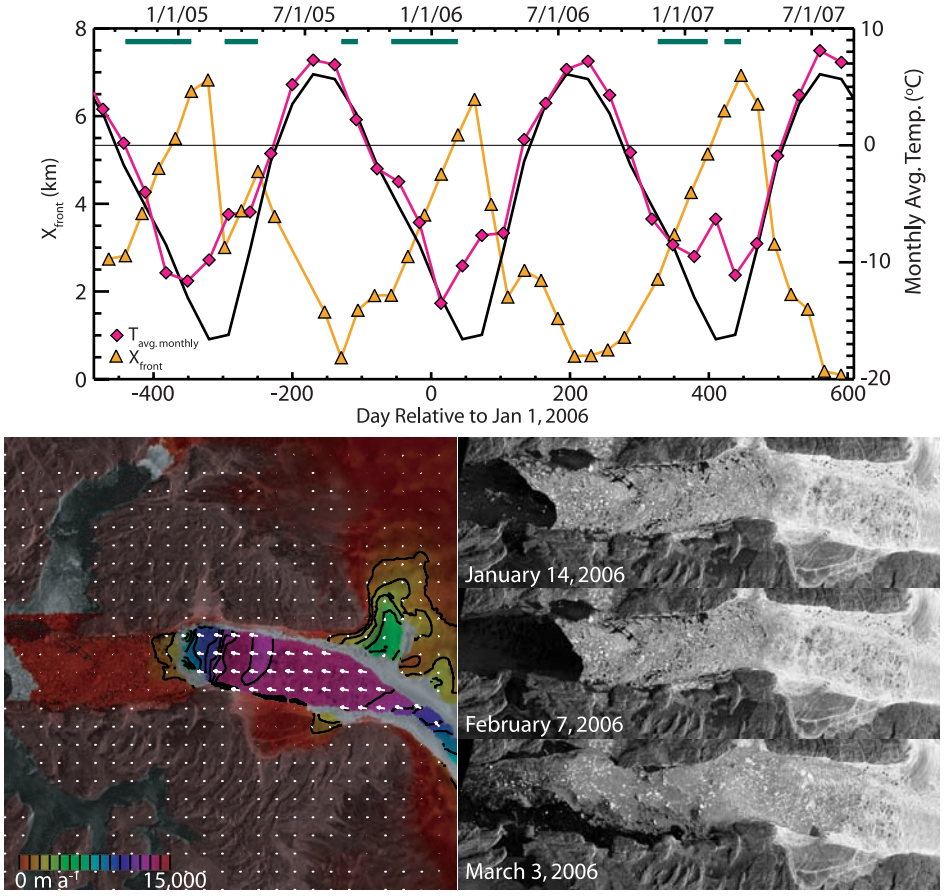

Figure 10. (top) Plot showing the ice front position from September 2004 to August 2007 (triangles). Also plotted is the mean monthly temperature (diamonds) along with 30-year monthly mean temperatures (cyclically repeated, solid black line). The solid green line shows the periods when the sikkusak moved "rigidly" in the fjord so that it could be speckle tracked. Gaps indicate no data, very rapid motion, or blocks of ice moving independently so they do not correlate. (left) Speed of the "rigid" ice as the ice front pushes it down the fjord. (right) Sequence of three images showing ice in the fjord as the calving front transitions from advance to retreat (see text).

side, the ice dam eventually broke mid- to late winter each year, causing rapid evacuation of much of the sikkusak from the fjord (Figure 10, March image). Once the confining sikkusak ice was removed, the ice front resumed rapid calving. In 2004 and to a lesser extent in 2005, the large volume of freshly calved ice following the initial "breakout" and the subfreezing conditions produced more sikkusak and a new constriction, which allowed the ice front to readvance prior to a second and final breakout. These observations strongly indicate that calving in winter is suppressed by the sikkusak, only to resume when this ice clears from the fjord or the sikkusak begins to behave nonrigidly. Since the formation of sea ice at the seaward end of the fjord likely would inhibit the clearing of the fjord, the timing of when open water is present in the fjord may control when the fjord clears and rapid calving begins.

[52] To investigate the role of sea ice further, Figure 11 shows winter temperatures at Egedesminde since 1980 along with the February, March, and April sea-ice concentrations for Disko Bay [*Stern and Heide-Jorgensen*, 2003]. From 1989 to 1996, there was nearly 100% sea-ice concentration in Disko Bay through much of the winter, and presumably in the adjacent fjord. This period of high sea-ice concentration corresponds well with the period when the glacier was thickening and moving at its slowest observed speed. This correspondence may result from reduced calving during periods of high sea-ice concentration that might have promoted thickening and increased buttressing by the ice tongue. Winter sea-ice concentration began to fall steadily over the next several years, to maximum concentrations of about 50–60% from 2003 onward, which is consistent with our observations of open water in the fjord from 2004 to 2007. Thus, both the longer seasonal duration and higher concentration of sea ice in the mid-1990s may have delayed when the ice cleared from the fjord.

[53] With the high speeds and calving rates at the ice front, an early clearing of the sikkusak from the fjord by a month or two when sea-ice concentration declined should have lengthened the calving season to produce an additional seasonal retreat of the ice front by 1 to 2 km. In 1998, 1 year after sea ice began to decline in Disko Bay, a retreat of this magnitude did occur and was followed by the eventual disintegration of the ice tongue and rapid speedup of the glacier [*Luckman and Murray*, 2005]. In contrast, a longer

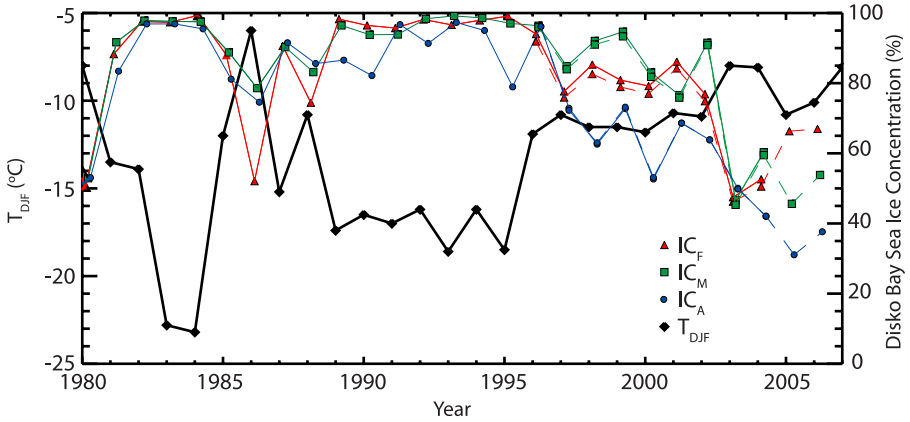

Figure 11. Winter/spring sea-ice concentration (color, right scale) in Disko Bay and winter (December–February) mean temperature at Egedesminde (black, left scale), 85 km southwest of where the fjord enters the bay.

sea-ice season may have suppressed calving, strengthening and thickening the shelf to yield slower velocities in the mid-1990s. We note that speeds on the glacier were also higher in 1985 when there was a brief period of reduced sea-ice concentration in Disko Bay, which is consistent with the above hypothesis. Thus, conditions that influence sea-ice growth in Disko Bay and in and around fjords in Greenland may exert a substantial control on outlet glacier stability. It also provides a mechanism for synchronous behavior over wide areas. For Disko Bay, sea-ice concentration correlates (∼0.6) with the North Atlantic Oscillation (NAO) index [*Stern and Heide-Jorgensen*, 2003]. Thus, the speedup on Jakobshavn and on many other glaciers over the last several years may be a response to changing climatic conditions related to a shift from a high NAO in the early to mid-1990s to more moderate values from the late 1990s onward [*Hurrell et al.*, 2003].

4.5. Future Evolution

[54] The initial speedup, which migrated rapidly inland over the fast moving areas, now appears to be progressing more gradually farther inland into slower moving ice. This is consistent with a diffusive process where the diffusion constant decreases with decreasing flow speed [*Bindschadler*, 1997]. Various models suggest that for a fixed perturbation, such as the loss of the ice tongue, the response should diffuse inland and eventually reach a new steady state [*Alley and Whillans*, 1984; *Bindschadler*, 1997; *Payne et al.*, 2004]. If the perturbation is fixed, then the downstream regions of Jakobshavn might rapidly (years to decades) approach a new steady state, with the more diffuse inland thinning taking longer to reequilibrate (decades to centuries). It is not clear, however, that the conditions near the ice front will remain fixed and instead they may continue to evolve to produce further thinning.

[55] While the bed topography is poorly known for Jakobshavn, the available data indicate the subglacial trough deepens inland of the current late summer ice front position, producing a reverse (upglacier dipping) bed slope [*Clarke and Echelmeyer*, 1996]. Several theoretical and model results indicate it is difficult for an outlet glacier to maintain a stable calving terminus on a reverse bed slope [*Schoof*, 2007; *Vieli et al.*, 2002]. Consistent with these predictions, many large outlet glaciers, such as Helheim Glacier in east Greenland, have retreated rapidly back over reversed bedrock slopes [*Howat et al.*, 2005, 2008b; *Moon and Joughin*, 2008]. In contrast, within our short window of observation and within the uncertainty of our sampling interval (16 to 24 days), Jakobshavn Isbrae's ice front has maintained a comparatively stable late summer position from 2004 to 2007, despite rapid thinning and continued speedup. In the cases of Jakobshavn Isbrae's 20th century retreat and the recent changes of Helheim Glacier, rapid retreat may have been facilitated by the limited ice flux that could be supplied through the narrow fjord's upper end. Jakobshavn Isbrae's late summer ice front is now embedded within the ice sheet, allowing strong additional inflow from the sides that may moderate thinning near the front and slow retreat [*Howat et al.*, 2007]. Along these lines, *Pfeffer* [2007] suggested that a calving terminus will remain stable as long as the ice thickness is large enough so that an ice thickness based stability index exceeds some critical threshold. Increased ice flux from the side could keep the ice thickness large enough to prevent accelerated retreat down the reverse slope.

[56] If inflow from the sides or some other process allows the ice front to maintain its current position, then it is likely that the glacier will begin to slow near the front as the ice in this region thins and flattens. While the difference is small (∼1 to 2% a^{-1}), the rate of speedup shown in Figure 4 already is greatest at some distance from the front (M20 and M26). If this is the case, then the glacier may already be stabilizing as it reaches a new equilibrium geometry.

[57] An alternative hypothesis is that rather than reaching a new equilibrium relatively quickly, the glacier might thin to the point where it can no longer maintain its stable ice front position. In this case, the instability associated with reverse bedrock slope might cause it to retreat along the deep trough that extends inland over 60 km well past the upstream end of the ATM grid, reaching depths in places of 1500 m below sea level [*Clarke and Echelmeyer*, 1996]. This process likely would be slowed by the need to draw down the surrounding kilometer thick ice on either side of the channel. Thus, this process of draw down as the front retreats, driven by reverse-sloped bed instability, may result

in a large negative mass balance persisting for several centuries.

5. Summary

[58] Following its rapid speedup that began in the late 1990s, Jakobshavn Isbrae is continuing to speed up and thin. The response of the glacier to the seasonal advance and retreat of the ice front significantly strengthens earlier hypotheses that indicated loss of the buttressing ice tongue as the main cause [*Joughin et al.*, 2004; *Thomas et al.*, 2003; *Thomas*, 2004]. Our analysis indicates this initial loss may have occurred when a trend toward reduced sea ice increased the duration of the calving season. If so, then sea ice may also play an important role in many of the recent speedups that have occurred since 2000 [*Joughin et al.*, 2004; *Thomas et al.*, 2003; *Thomas*, 2004].

[59] While our data give some idea as to how the Jakobshavn drainage basin will respond, it is still unclear how rapidly a new steady state will be achieved. Numerical ice sheet models such as those that have been applied to other glaciers [e.g., *Payne et al.*, 2004; *Vieli et al.*, 2001] could improve predictions of the glacier's response and its contribution to sea level. Continued measurement of the evolving flow field, geophysical efforts to define the fjord geometry more precisely, and improved understanding of ocean/fjord/ice interactions will all improve our collective ability to model this and similar systems.

[60] **Acknowledgments.** The National Science Foundation (NSF) supported contributions by I. Joughin (ARC0531270), M. Fahnestock (ARC0531250), R. Alley (ARC0531211), H. Stern (ARC0531133), and M. Truffer (ARC0531075) through Arctic System Science Grants. The National Aerospace Administration supported I. Howat's, B. Smith's (NNG06GE5SG), and W. Krabill's contributions. Work by R. Alley was also partially supported by NSF 0424589 and NASA NNG06GB37G. The RADARSAT data were acquired by the Canadian Space Agency and downlinked and distributed by the Alaska Satellite Facility. Comments by G. Hamilton, A. Vieli, B. Csatho, and an anonymous reviewer led to substantial improvements in the final manuscript.

References

Alley, R. B., and I. M. Whillans (1984), Response of the east Antarctica ice-sheet to sea-level rise, *J. Geophys. Res.*, *89*(C4), 6487–6493, doi:10.1029/JC089iC04p06487.

Alley, R. B., P. U. Clark, P. Huybrechts, and I. Joughin (2005), Ice-sheet and sea-level changes, *Science*, *310*(5747), 456–460, doi:10.1126/science.1114613.

Bamber, J. L., S. Ekholm, and W. B. Krabill (2001), A new, high-resolution digital elevation model of Greenland fully validated with airborne laser altimeter data, *J. Geophys. Res.*, *106*(B4), 6733–6745, doi:10.1029/2000JB900365.

Bindschadler, R. (1997), Actively surging west Antarctic ice streams and their response characteristics, *Ann. Glaciol.*, *24*, 409–414.

Bindschadler, R. A. (1984), Jakobshavn Glacier drainage basin: A balance assessment, *J. Geophys. Res.*, *89*(C2), 2066–2072, doi:10.1029/JC089iC02p02066.

Clarke, T. S., and K. Echelmeyer (1996), Seismic-reflection evidence for a deep subglacial trough beneath Jakobshavns Isbrae, west Greenland, *J. Glaciol.*, *42*(141), 219–232.

Csatho, B., T. Schenk, C. J. Van der Veen, and W. B. Krabill (2008), Intermittent thinning of Jakobshavn Isbrae, west Greenland, since the Little Ice Age, *J. Glaciol.*, *54*(184), 131–144, doi:10.3189/002214308784409035.

Das, S. B., I. Joughin, M. D. Behn, I. M. Howat, M. A. King, D. Lizarralde, and M. P. Bhatia (2008), Fracture propagation to the base of the Greenland Ice Sheet during supraglacial lake drainage, *Science*, *320*(5877), 778–781, doi:10.1126/science.1153360.

Dietrich, R., H. G. Maas, M. Baessler, A. Ruelke, A. Richter, E. Schwalbe, and P. Westfeld (2007), Jakobshavn Isbrae, west Greenland: Flow velocities and tidal interaction of the front area from 2 004 field observations, *J. Geophys. Res.*, *112*, F03S21, doi:10.1029/2006JF000601.

Dupont, T. K., and R. B. Alley (2005), Assessment of the importance of ice-shelf buttressing to ice-sheet flow, *Geophys. Res. Lett.*, *32*, L04503, doi:10.1029/2004GL022024.

Echelmeyer, K., and W. D. Harrison (1990), Jakobshavns Isbrae, west Greenland: Seasonal variations in velocity or lack thereof, *J. Glaciol.*, *36*(122), 82–88.

Echelmeyer, K., T. S. Clarke, and W. D. Harrison (1991), Surficial glaciology of Jakobshavns Isbrae, west Greenland. Part 1. Surface morphology, *J. Glaciol.*, *37*(127), 368–382.

Fastook, J. L., H. H. Brecher, and T. J. Hughes (1995), Derived bedrock elevations, strain rates and stresses from measured surface elevations and velocities: Jakobshavns Isbrae, Greenland, *J. Glaciol.*, *41*(137), 161–173.

Goldsby, D. L., and D. L. Kohlstedt (2001), Superplastic deformation of ice: Experimental observations, *J. Geophys. Res.*, *106*(B6), 11,017–11,030, doi:10.1029/2000JB900336.

Howat, I. M., I. Joughin, S. Tulaczyk, and S. Gogineni (2005), Rapid retreat and acceleration of Helheim Glacier, east Greenland, *Geophys. Res. Lett.*, *32*, L22502, doi:10.1029/2005GL024737.

Howat, I. M., I. Joughin, and T. A. Scambos (2007), Rapid changes in ice discharge from Greenland outlet glaciers, *Science*, *315*(5818), 1559–1561, doi:10.1126/science.1138478.

Howat, I. M., B. E. Smith, I. Joughin, and T. A. Scambos (2008a), Rates of mass-loss from southeast Greenland from combined ICESAT and ASTER observations, *Geophys. Res. Lett.*, *35*, L17505, doi:10.1029/2008GL034496.

Howat, I. M., I. Joughin, M. Fahnestock, B. E. Smith, and T. Scambos (2008b), Synchronous retreat and acceleration of southeast Greenland outlet glaciers 2000–2006: Ice dynamics and coupling to climate, *J. Glaciol.*, *54*(187), 646–660.

Hurrell, J. W., Y. Kushnir, M. M. Visbeck, and G. G. Ottersen (2003), An overview of the North Atlantic Oscillation, in *The North Atlantic Oscillation: Climate Significance and Environmental Impact*, *Geophys. Monogr. Ser.*, vol. 134, edited by J. W. Hurrell et al., pp. 1–35, AGU, Washington, D. C.

Jennings, A. E., and N. J. Weiner (1996), Environmental change in eastern Greenland during the last 1300 years: Evidence from foraminifera and lithofacies in Nansen Fjord, 68(N, *Holocene*, *6*(2), 179–191, doi:10.1177/095968369600600205.

Joughin, I. (2002), Ice-sheet velocity mapping: A combined interferometric and speckle-tracking approach, *Ann. Glaciol.*, *34*, 195–201, doi:10.3189/172756402781817978.

Joughin, I. R., R. Kwok, and M. A. Fahnestock (1998), Interferometric estimation of three-dimensional ice-flow using ascending and descending passes, *IEEE Trans. Geosci. Remote Sens.*, *36*(1), 25–37, doi:10.1109/36.655315.

Joughin, I., E. Rignot, C. E. Rosanova, B. K. Lucchitta, and J. Bohlander (2003), Timing of recent accelerations of Pine Island Glacier, Antarctica, *Geophys. Res. Lett.*, *30*(13), 1706, doi:10.1029/2003GL017609.

Joughin, I., W. Abdalati, and M. Fahnestock (2004), Large fluctuations in speed on Greenland's Jakobshavn Isbrae Glacier, *Nature*, *432*(7017), 608–610, doi:10.1038/nature03130.

Joughin, I., S. B. Das, M. A. King, B. E. Smith, I. M. Howat, and T. Moon (2008a), Seasonal speedup along the western flank of the Greenland Ice Sheet, *Science*, *320*(5877), 781–783, doi:10.1126/science.1153288.

Joughin, I., I. M. Howat, R. B. Alley, G. Ekstrom, M. Fahnestock, T. Moon, M. Nettles, M. Truffer, and V. C. Tsai (2008b), Ice-front variation and tidewater behavior on Helheim and Kangerdlugssuaq glaciers, Greenland, *J. Geophys. Res.*, *113*, F01004, doi:10.1029/2007JF000837.

Krabill, W., E. Frederick, S. Manizade, C. Martin, J. Sonntag, R. Swift, R. Thomas, W. Wright, and J. Yungel (1999), Rapid thinning of parts of the southern Greenland Ice Sheet, *Science*, *283*(5407), 1522–1524, doi:10.1126/science.283.5407.1522.

Krabill, W., et al. (2000), Greenland Ice Sheet: High-elevation balance and peripheral thinning, *Science*, *289*(5478), 428–430, doi:10.1126/science.289.5478.428.

Krabill, W., et al. (2004), Greenland Ice Sheet: Increased coastal thinning, *Geophys. Res. Lett.*, *31*, L24402, doi:10.1029/2004GL021533.

Luckman, A., and T. Murray (2005), Seasonal variation in velocity before retreat of Jakobshavn Isbrae, Greenland, *Geophys. Res. Lett.*, *32*, L08501, doi:10.1029/2005GL022519.

Luckman, A., T. Murray, R. de Lange, and E. Hanna (2006), Rapid and synchronous ice-dynamic changes in east Greenland, *Geophys. Res. Lett.*, *33*, L03503, doi:10.1029/2005GL025428.

Luthi, M., M. Funk, A. Iken, S. Gogineni, and M. Truffer (2002), Mechanisms of fast flow in Jakobshavn Isbrae, west Greenland: Part III. Measurements of ice deformation, temperature and cross-borehole conductivity in boreholes to the bedrock, *J. Glaciol.*, *48*(162), 369–385, doi:10.3189/172756502781831322.

Moon, T., and I. Joughin (2008), Changes in ice front position on Greenland's outlet glaciers from 1992 to 2007, *J. Geophys. Res.*, *113*, F02022, doi:10.1029/2007JF000927.

Paterson, W. S. B. (1994), *The Physics of Glaciers*, 3rd ed., 480 pp., Pergamon, Oxford, U. K.

Payne, A. J., A. Vieli, A. P. Shepherd, D. J. Wingham, and E. Rignot (2004), Recent dramatic thinning of largest west Antarctic ice stream triggered by oceans, *Geophys. Res. Lett.*, *31*, L23401, doi:10.1029/2004GL021284.

Pfeffer, W. T. (2007), A simple mechanism for irreversible tidewater glacier retreat, *J. Geophys. Res.*, *112*, F03S25, doi:10.1029/2006JF000590.

Reeh, N., H. H. Thomsen, A. K. Higgins, and A. Weidick (2001), Sea ice and the stability of north and northeast Greenland floating glaciers, *Ann. Glaciol.*, *33*, 474–480, doi:10.3189/172756401781818554.

Rignot, E., and P. Kanagaratnam (2006), Changes in the velocity structure of the Greenland Ice Sheet, *Science*, *311*(5763), 986–990, doi:10.1126/science.1121381.

Scambos, T. A., C. Hulbe, M. Fahnestock, and J. Bohlander (2000), The link between climate warming and break-up of ice shelves in the Antarctic Peninsula, *J. Glaciol.*, *46*(154), 516–530, doi:10.3189/172756500781833043.

Schoof, C. (2005), The effect of cavitation on glacier sliding, *Proc. R. Soc. London Ser. A*, *461*(2055), 609–627.

Schoof, C. (2007), Ice sheet grounding line dynamics: Steady states, stability, and hysteresis, *J. Geophys. Res.*, *112*, F03S28, doi:10.1029/2006JF000664.

Sohn, H. G., K. C. Jezek, and C. J. van der Veen (1998), Jakobshavn Glacier, west Greenland: 30 years of spaceborne observations, *Geophys. Res. Lett.*, *25*(14), 2699–2702, doi:10.1029/98GL01973.

Stern, H. L., and M. P. Heide-Jorgensen (2003), Trends and variability of sea ice in Baffin Bay and Davis Strait, 1953–2001, *Polar Res.*, *22*(1), 11–18, doi:10.1111/j.1751-8369.2003.tb00090.x.

Thomas, R. H. (2004), Force-perturbation analysis of recent thinning and acceleration of Jakobshavn Isbrae, Greenland, *J. Glaciol.*, *50*(168), 57–66, doi:10.3189/172756504781830321.

Thomas, R. H., W. Abdalati, E. Frederick, W. B. Krabill, S. Manizade, and K. Steffen (2003), Investigation of surface melting and dynamic thinning on Jakobshavn Isbrae, Greenland, *J. Glaciol.*, *49*(165), 231–239, doi:10.3189/172756503781830764.

Tsai, V. C., and G. Ekstrom (2007), Analysis of glacial earthquakes, *J. Geophys. Res.*, *112*, F03S22, doi:10.1029/2006JF000596.

van der Veen, C. J. (1998a), Fracture mechanics approach to penetration of bottom crevasses on glaciers, *Cold Reg. Sci. Technol.*, *27*(3), 213–223, doi:10.1016/S0165-232X(98)00006-8.

van der Veen, C. J. (1998b), Fracture mechanics approach to penetration of surface crevasses on glaciers, *Cold Reg. Sci. Technol.*, *27*(1), 31–47, doi:10.1016/S0165-232X(97)00022-0.

van de Wal, R. S. W., W. Greuell, M. Van den Broeke, C. H. Reijmer, and J. Oerlemans (2005), Surface mass-balance observations and automatic weather station data along a transect near Kangerlussuaq, west Greenland, *Ann. Glaciol.*, *42*, 311–316, doi:10.3189/172756405781812529.

Vieli, A., M. Funk, and H. Blatter (2001), Flow dynamics of tidewater glaciers: A numerical modelling approach, *J. Glaciol.*, *47*(159), 595–606, doi:10.3189/172756501781831747.

Vieli, A., J. Jania, and L. Kolondra (2002), The retreat of a tidewater glacier: Observations and model calculations on Hansbreen, Spitsbergen, *J. Glaciol.*, *48*(163), 592–600, doi:10.3189/172756502781831089.

Weertman, J. (1983), Creep deformation of ice, *Annu. Rev. Earth Planet. Sci.*, *11*, 215–240, doi:10.1146/annurev.ea.11.050183.001243.

Weidick, A. (1995), *Satellite image atlas of glaciers of the world—Greenland*, *Prof. Pap. 1386-C*, U. S. Geol. Surv., Reston, Va.

Zwally, H. J., W. Abdalati, T. Herring, K. Larson, J. Saba, and K. Steffen (2002), Surface melt-induced acceleration of Greenland Ice Sheet flow, *Science*, *297*(5579), 218–222, doi:10.1126/science.1072708.

R. B. Alley, Department of Geosciences, and Earth and Environmental Systems Institute, Pennsylvania State University, University Park, PA 16802, USA. (rba6@psu.edu)

M. Fahnestock, Institute for the Study of Earth, Oceans, and Space, University of New Hampshire, Morse Hall, 8 College Road, Durham, NH 03824-3525, USA.

I. M. Howat, Byrd Polar Research Center, School of Earth Sciences, Ohio State University, Scott Hall Room 108, 1090 Carmack Road, Columbus, OH 43210-1002, USA.

I. Joughin, B. Smith, and H. Stern, Applied Physics Laboratory, Polar Science Center, University of Washington, 1013 NE 40th Street, Seattle, WA 98105-6698, USA. (ian@apl.washington.edu)

W. Krabill, Cryospheric Sciences Branch, Wallops Flight Facility, Goddard Space Flight Center, NASA, Code 614.1, Wallops Island, VA 23337, USA.

M. Truffer, Geophysical Institute, University of Alaska Fairbanks, 903 Koyukuk Drive, Fairbanks, AK 99775-7320, USA.